Encoder-Decoder Network with Guided Transmission Map: Robustness and Applicability

Le-Anh Tran and Dong-Chul Park

Myongji University, Yongin, South Korea
leanhtran@mju.ac.kr, parkd@mju.ac.kr

Abstract. The robustness and applicability of the Encoder-Decoder Network with Guided Transmission Map (EDN-GTM) proposed for efficient single image dehazing purpose are examined in this paper. The EDN-GTM utilizes the transmission map extracted by dark channel prior approach as an additional input channel of a novel U-Net-based generative network to achieve an improved dehazing performance. The EDN-GTM has shown a very favorable performance compared with most recently proposed dehazing schemes including both traditional and deep learning-based ones in terms of PSNR and SSIM metrics. To further validate the robustness and applicability of the EDN-GTM scheme, extensive experiments and quantitative evaluations on various benchmark datasets are conducted in this paper. In terms of robustness, experimental results on different benchmark dehazing datasets such as Dense-HAZE, NH-HAZE, and D-HAZY show that the EDN-GTM scheme consistently outperforms most modern dehazing approaches on both synthetic and realistic hazy data regardless of scene locations: indoor or outdoor. On the other hand, experiments on WAYMO and Foggy Driving datasets imply that the EDN-GTM can be effectively applied as an image preprocessing tool to object detection tasks in autonomous driving systems.

Keywords: image dehazing, dark channel prior, spatial pyramid pooling, U-Net, object detection

1 Introduction

Deterioration of the digital image quality negatively affects the performance of various vision-based tasks including object detection in autonomous driving systems. Typically, haze can be considered one of the most frequently experienced natural phenomena causing image visibility degradation. Accurate estimation of the transmission map in a hazy image, however, has been a major obstacle in performing haze removal or dehazing [1]. Numerous single image dehazing approaches have been proposed in attempt to enhance the visibility of hazy images and some of them have achieved significant progress. Generally, dehazing algorithms can be categorized into two genres: traditional methods and deep learning-based methods.

In terms of traditional approaches, Meng *et al.* [2] have proposed an efficient dehazing method by enforcing the boundary constraint and contextual regularization for sharper restored images. Zhu *et al.* [3] have developed a color attenuation prior (CAP) that creates a linear model for modeling the scene depth of hazy image and learns the parameters of the model with a supervised learning manner. Noticeably, He *et al.* [4] have proposed the dark channel prior (DCP) which is developed based on the statistics of haze-free outdoor images to directly estimate the haze thickness and the dehazed image is derived subsequently using the haze imaging model.

On the other hand, convolutional neural networks (CNNs) have been gradually replacing traditional handcrafted graphical models. Cai *et al.* [5] have introduced DehazeNet which predicts the medium transmission map from hazy image and haze-free image is restored subsequently based on the atmospheric scattering model. Ren *et al.* [6] have proposed a multi-scale CNN (MSCNN) which consists of a coarse-scale network for predicting a holistic transmission map and a fine-scale network for refining the result locally. Unlike aforementioned approaches that consider only the prediction of transmission map, Li *et al.* [1] have proposed an all-in-one dehazing network (AOD-Net) which directly learns the mapping between hazy image and haze-free image. In addition to conventional CNNs, several studies have adopted generative adversarial networks (GANs) for image dehazing and have shown promising results. Dong *et al.* [7] have proposed a GAN model with fusion-discriminator (FD-GAN) which takes frequency information as an additional prior and is able to generate more natural-looking dehazed images with less color distortion.

In order to take advantage of both traditional and deep learning-based approaches, the Encoder-Decoder Network with Guided Transmission Map (EDN-GTM) has been proposed in [8] which utilizes the transmission map extracted by DCP as an additional input channel of a novel U-Net-based generative network to achieve an improved dehazing performance. To further validate the robustness and applicability of the EDN-GTM scheme to other computer vision tasks, extensive experiments on various image scenes and different types of hazy data with the EDN-GTM scheme and some of the most highly accepted image dehazying algorithms are conducted and the results with performance comparison are reported in this paper.

The rest of this paper is organized as follows: Section 2 briefly reviews the EDN-GTM scheme. A data preparation process for our experiments is presented in Section 3. In Section 4, extensive experiments on different types of hazy data in various image scenes with the EDN-GTM and other image dehazing schemes are conducted and the performance comparison results are summarized. Finally, Section 5 concludes the paper.

2 The EDN-GTM Scheme

The transmission map in atmospheric scattering model has a very close relationship with the depth information which benefits many vision applications

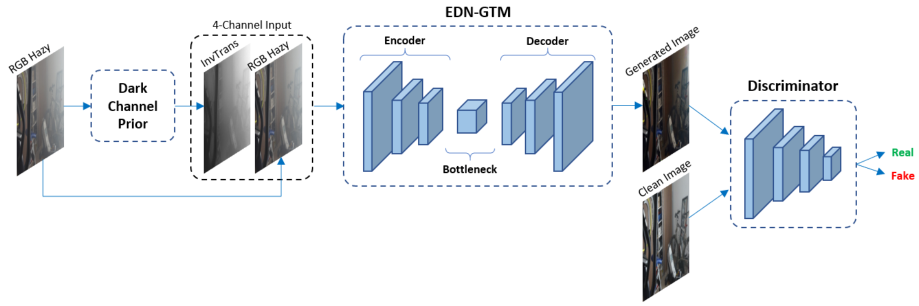

Fig. 1. The EDN-GTM scheme.

such as image-based learning models like CNNs [8]. The EDN-GTM utilizes the transmission map estimated by DCP as an additional input channel for a CNN model to achieve an improved dehazing performance. In addition, the EDN-GTM adopts U-Net as the core network because it is widely considered one of the most powerful encoder-decoder networks applied to image restoration and segmentation purposes [9]. To further upgrade U-Net for dehazing task, three main modifications are carried out [8]: 1) a spatial pyramid pooling (SPP) module is plugged into the bottleneck to increase the receptive field and separate out the significant context features [10]; 2) ReLU activation is replaced with Swish activation because Swish function has been shown to consistently outperform ReLU function on deep networks [11]; 3) one convolution layer with the size of 3x3 is appended to each of the main convolution stages to increase the receptive field and capture more high-level features from larger regions in the input image. In terms of optimization function, the EDN-GTM applies an integral loss function [8] which is a weighted sum of adversarial loss, MSE loss, and perceptual loss for the sake of both pixel quality and human perception. The overall diagram of the EDN-GTM scheme is illustrated in Fig. 1.

3 Data Preparation

3.1 Atmospheric Scattering Model

The atmospheric scattering model used for the description of a hazy image is expressed as [1]:

$$I(x) = J(x)t(x) + A(1 - t(x)) \tag{1}$$

where $I(x)$, $J(x)$, A, and $t(x)$ denote the observed intensity, the scene radiance, the global atmospheric light, and the transmission map, respectively. When the atmospheric light is homogenous, $t(x)$ can be expressed as [1]:

$$t(x) = e^{-\beta d(x)} \tag{2}$$

Fig. 2. Synthesized hazy images from WAYMO dataset: (a) Clean images, (b) Synthesized hazy images by the proposed method, and (c) Synthesized hazy images based on random transmission map.

where β represents the scattering coefficient of the atmosphere, and $d(x)$ is the scene depth.

3.2 Synthesizing Hazy Data for Driving Object Detection

In order to obtain synthetic hazy data to be used as training dataset, one of the simplest methods is applying random transmission maps to (1) to generate synthetic hazy images [5] [6]. However, this method may not be valid in some cases where the images contain complex scenes or dark scenes, this incident can lead to creating unreliable training image samples [20]. Apart from that simple method, we propose a novel procedure that applies (2) to estimate the transmission map instead of randomizing it in attempt to obtain a more accurate transmission map, thereby resulting in obtaining more natural-looking synthetic hazy images.

Specifically, a pre-trained Monodepth2 model [12] which was trained on driving image data is applied to estimate the scene depth. When the scene depth is derived, (2) and (1) are sequentially applied to generate transmission map and synthetic hazy image. In order to avoid generating only a certain amount of haze in all images, the value of β in (2) is set to be a randomly chosen number between 1.0 to 3.0. This selection method of β can generate different degrees of haze in the synthesized image data and can enhance the diversity of training data. Fig. 2 shows an illustration of several synthesized hazy data from WAYMO dataset [13] by adopting the proposed method. As can be seen from Fig. 2, we can obtain more natural-looking hazy images by applying the proposed method than those of the method based on random transmission maps.

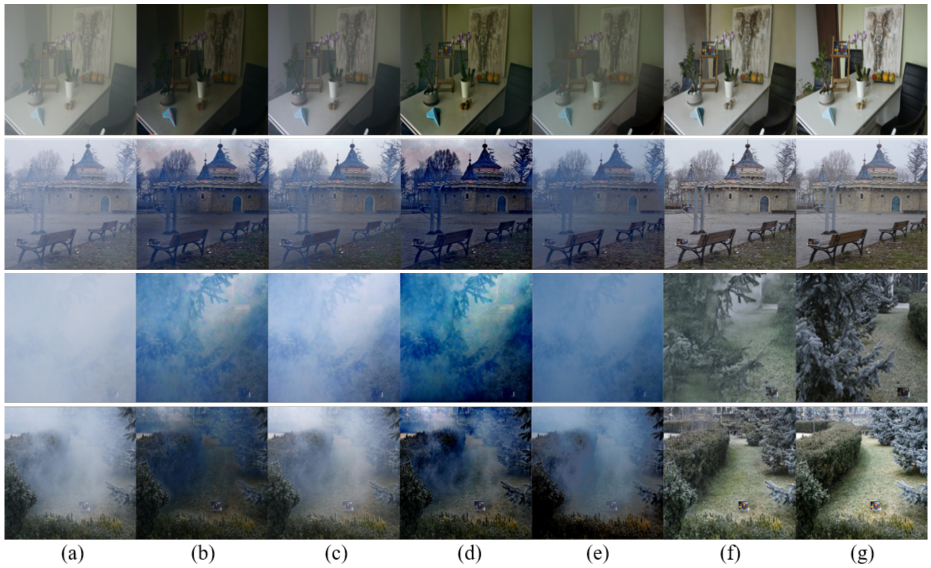

Fig. 3. Visual dehazing results on high-resolution realistic hazy datasets: (a) Input, (b) DCP [4], (c) CAP [3], (d) Meng *et al.* [2], (e) AOD-Net [1], (f) EDN-GTM, and (g) Ground Truth (from top to bottom, representative validation data of I-HAZE, O-HAZE, Dense-HAZE, and NH-HAZE datasets, respectively).

3.3 Datasets

Dehazing Datasets To validate of the robustness of the EDN-GTM scheme, five benchmark datasets with different types of haze data in indoor and outdoor scenes are utilized to conduct experiments:

- I-HAZE and O-HAZE [14]: These datasets contain 25 and 35 pairs of corresponding hazy and haze-free images of indoor and outdoor scenes for training, respectively, and both contain 5 image pairs for validation. The images are provided in high resolution and have an average size of approximately 2,800x4,600 pixels.
- Dense-HAZE [15]: This dataset is known as one of the most challenging datasets in dehazing tasks with image data containing dense and heavy haze. The dataset contains 45 pairs of hazy and haze-free images for training and 5 image pairs for validation. The image size is $1{,}200 \times 1{,}600$ pixels.
- NH-HAZE [15]: This dataset provides non-homogeneous hazy image data and contains 45 hazy and haze-free image pairs with 40 image pairs for training and the remaining 5 image pairs for validation. The image size in this dataset is $1{,}200 \times 1{,}600$ pixels.
- D-HAZY [16]: This is a benchmark synthetic dehazing dataset with 1,449 pairs of clean and synthetic hazy images of indoor scenes.

Table 1. Quantitative dehazing results on I-HAZE and O-HAZE datasets.

	I-HAZE		O-HAZE	
Method	**PSNR**	**SSIM**	**PSNR**	**SSIM**
DCP (TPAMI'10) [4]	14.43	0.7516	16.78	0.6532
CAP (TIP'15) [3]	12.24	0.6065	16.08	0.5965
MSCNN (ECCV'16) [6]	15.22	0.7545	17.56	0.6495
AOD-Net (ICCV'17) [1]	13.98	0.7323	15.03	0.5385
PPD-Net (CVPRW'18) [14]	22.53	0.8705	24.24	0.7205
EDN-GTM	22.90	0.8270	23.46	0.8198

Table 2. Quantitative dehazing results on Dense-HAZE and NH-HAZE datasets.

	Dense-HAZE		NH-HAZE	
Method	**PSNR**	**SSIM**	**PSNR**	**SSIM**
DCP (TPAMI'10) [4]	10.06	0.3856	10.57	0.5196
DehazeNet (TIP'16) [5]	13.84	0.4252	16.62	0.5238
AOD-Net (ICCV'17) [1]	13.14	0.4144	15.40	0.5693
MSBDN (CVPR'20) [18]	15.37	0.4858	19.23	0.7056
AECR-Net (CVPR'21) [15]	15.80	0.4660	19.88	0.7173
EDN-GTM	15.43	0.5200	20.24	0.7178

Object Detection Datasets In order to prove the applicability of the EDN-GTM scheme to object detection module in autonomous driving systems [21], two benchmark datasets are chosen to examine in our experiments:

– WAYMO [13]: This dataset provides a benchmark for 2D object detection tasks in driving scenarios with approximately 100K images. However, only 1,100 images are utilized to conduct dehazing and object detection experiments. Specifically, 1,000 and 100 front-view images for training and validation, respectively.
– Foggy Driving [17]: The dataset consists of natural foggy driving scenes which is a benchmark for evaluating object detection performance on real-world foggy scenes. Because this dataset does not provide pairs of foggy-clean images for supervised training, we apply directly the pre-trained weights of the EDN-GTM which is trained on the synthesized hazy images of WAYMO dataset to perform haze removal on Foggy Driving dataset.

4 Results on Benchmark Datasets and Applications to Driving Object Detection Tasks

This section provides the performances of the EDN-GTM scheme on different types of hazy data in various image scenes. The dehazing performance is mea-

Fig. 4. Visual dehazing results of the EDN-GTM on synthetic hazy dataset D-HAZY (top: hazy images, middle: dehazed images, bottom: ground truth images).

Table 3. Quantitative dehazing results on D-HAZY dataset.

Method	PSNR	SSIM	Time (sec.)
DCP (TPAMI'10) [4]	14.4794	0.8280	0.17
CAP (TIP'15) [3]	14.7497	0.8145	0.20
DehazeNet (TIP'16) [5]	14.7265	0.8199	0.09
MSCNN (ECCV'16) [6]	13.6193	0.7865	0.14
C2MSNet (WACV'18) [19]	16.5808	0.8480	0.072
EDN-GTM	24.0366	0.8914	0.085

sured by using peak signal-to-noise ratio (PSNR) and structural similarity index measure (SSIM) metrics. The PSNR, however, is chosen as our primary performance measure because we consider the quality of pixel restoration to be the utmost factor so that the scheme can benefit other computer vision tasks such as object detection.

4.1 Dehazing Results on Realistic Haze Datasets

The performances of the EDN-GTM scheme on I-HAZE and O-HAZE datasets are first compared with those of other approaches in Table 1. As shown in Table 1, on I-HAZE dataset, the EDN-GTM scheme achieves the best dehazing performance in terms of PSNR (22.90 dB) while showing the second-best performance in terms of SSIM (0.8270). On O-HAZE dataset, the EDN-GTM scheme gives the second-best performance in terms of PNSR (23.46 dB) while showing the best performance in terms of SSIM (0.8198). More quantitative dehazing results

Fig. 5. Visual dehazing results on synthesized hazy data (in each pair, the left image denotes the hazy image and the right image presents the dehazed image).

on I-HAZE and O-HAZE datasets are summarized in Table 1, where the best and the second-best results are shown in red and blue colors, respectively.

Experiments on Dense-HAZE and NH-HAZE datasets are then performed. Note that Dense-HAZE and NH-HAZE datasets are more challenging than I-HAZE and O-HAZE datasets. The performances of the EDN-GTM scheme are also compared with those of other approaches and summarized in Table 2, where the best and the second-best results are shown in red and blue colors, respectively. On Dense-HAZE dataset, the EDN-GTM scheme gives the second-best performance in terms of PNSR (15.43 dB) while showing the best performance in terms of SSIM (0.5200). On NH-HAZE dataset, the EDN-GTM scheme convincingly achieves the best dehazing performance in both PSNR (20.24 dB) and SSIM (0.7178).

Typical visual dehazing results of the EDN-GTM scheme and other methods on four benchmark realistic dehazing datasets including I-HAZE, O-HAZE, Dense-HAZE and NH-HAZE datasets are shown in Fig. 3. As can be seen from Fig. 3, the EDN-GTM can produce more visually compelling dehazed images compared to those of other modern haze removal algorithms.

As the qualitative and quantitative evaluations shown in Fig. 3, Table 1 and Table 2, the EDN-GTM scheme achieves very favorable results on all the datasets in our experiments when compared with other recent dehazing methods. The qualitative and quantitative results demonstrate that the EDN-GTM scheme has a well-designed architecture that can perform efficiently on haze removal tasks. In addition, we notice that transmission map plays a very important role in guiding the EDN-GTM scheme to produce excellent results in image dehazing tasks.

4.2 Dehazing Results on Synthetic Hazy Dataset

Further experiments on benchmark synthetic dataset, D-HAZY [16], are also carried out to prove the robustness of the EDN-GTM scheme on synthetic hazy image data. In our experiment, D-HAZY dataset is first splitted into training

Fig. 6. Application of the EDN-GTM scheme to object detection on WAYMO dataset. In each pair, the left image denotes the hazy image and the right image presents the dehazed image (red box: ground truth, green box: detection).

Table 4. Improvement of the detection accuracy on synthesized hazy WAYMO Dataset using EDN-GTM.

	Hazy Images	**Dehazed Images**
mAP	41.91%	**46.64%**

set (807 images) and validation set (642 images) because D-HAZY dataset does not divide its data for training and testing beforehand [19]. We also consider the inference time of the EDN-GTM in comparison with that of other dehazing methods to investigate the execution speed of the EDN-GTM. As indicated in Table 3 where the best results are indicated in red numbers and blue numbers demonstrate the second-best results, the EDN-GTM achieves the best performance in both PSNR and SSIM while its inference time is still competitive against other approaches with the second-best result, 0.085 seconds per image. Fig. 4 shows several visual dehazing results of the EDN-GTM scheme on D-HAZY dataset, where the top, the middle, and the bottom images denote the input hazy, the dehazed, and the ground truth images, respectively.

4.3 Object Detection Results on Synthetic Hazy Driving Scenes

In order to evaluate the applicability of the EDN-GTM scheme to driving object detection problems, the scheme is utilized as a pre-processing tool of hazy images. Visual dehazing results on synthesized WAYMO hazy dataset are indicated

Fig. 7. Visual dehazing results on natural foggy images in Foggy Driving dataset produced by the EDN-GTM scheme (in each pair, the left image denotes the hazy image and the right image presents the dehazed image).

Table 5. Improvement of the detection accuracy on Foggy Driving Dataset using EDN-GTM.

	Hazy Image Set	**Dehazed Image Set**
mAP	77.88%	**79.08%**

in Fig. 5. After haze removal is performed on the input images by adopting the EDN-GTM scheme, a pre-trained YOLOv4 object detection model [10] which was trained on the original WAYMO dataset is utilized to evaluate object detection performances on hazy and dehazed images. The experimental results are summarized in Table 4. As shown in Table 4, the EDN-GTM scheme helps to increase the mean average precision (mAP) by 4.73% which is 11.3% improvement over the system without the pre-processing step performed by the EDN-GTM scheme. Fig. 6 shows visual detection results on hazy and dehazed images, where the red and green boxes indicate the ground truth objects and the detected objects, respectively. As can be seen from Fig. 6, the dehazed images obtained through the EDN-GTM scheme can provide much improved detection results than what the original hazy images can provide.

4.4 Object Detection Results on Natural Hazy Driving Scenes

In order to investigate the robustness and applicability of the EDN-GTM scheme to object detection in natural foggy driving scenes, the performance of the EDN-GTM scheme on Foggy Driving dataset [17] is also examined. The pre-trained

Fig. 8. Application of the EDN-GTM scheme to object detection on Foggy Driving dataset. In each pair, the left image denotes the hazy image and the right image presents the dehazed image (red box: ground truth, green box: detection).

EDN-GTM model which was trained on synthesized WAYMO hazy data is first utilized to perform dehazing on Foggy Driving dataset. As can be seen from Fig. 7 for the visual dehazing results, the EDN-GTM scheme can remove the haze significantly and the restored scenes are much cleaner that endow great support to the vision of the driver or the camera of autonomous driving systems. The experimental results may consolidate that the EDN-GTM scheme can be considered a robust tool for natural haze removal. The results shown in Fig. 7 imply that the EDN-GTM scheme can help even human drivers under foggy weather conditions. Note that the model used in this experiment was trained on synthesized hazy WAYMO dataset but was tested on natural hazy Foggy Driving dataset. Hence, this result also demonstrates that the strategy of using synthesized hazy data for training the EDN-GTM scheme when natural foggy images are limited is very excellent and has high potential. In addition, the proposed method for synthesizing hazy data is very promising.

The experimental results of object detection performance using the EDN-GTM scheme on Foggy Driving dataset are summarized in Table 5. A pre-trained YOLOv4 model is utilized to evaluate object detection performances on original and dehazed images. The quantitative results shown in Table 5 demonstrate that the EDN-GTM scheme can help to improve the accuracy of object detection from 77.88% to 79.08% in mAP. Typical visual results of object detection can be seen in Fig. 8. The results in Fig. 8 show that the EDN-GTM scheme has a potential to help the object detection tasks in obtaining better localization results, reducing false positives, and improving detection accuracy on distant and small objects. As a result, the EDN-GTM scheme can be considered an efficient image enhancement tool for foggy images.

5 Conclusions

In this paper, the robustness and applicability of the Encoder-Decoder Network with Guided Transmission Map (EDN-GTM) proposed for effective single image dehazing are presented. The EDN-GTM combines the transmission map extracted by dark channel prior algorithm with an upgraded architecture of U-Net developed for dehazing task in order to achieve an improved dehazing performance. To validate the robustness of the EDN-GTM scheme, extensive experiments on various image scenes and different types of hazy data are conducted and the results have shown that the EDN-GTM scheme consistently outperforms most recent dehazing methods in terms of PSNR and SSIM metrics. In addition, the applicability of the EDN-GTM scheme is verified when it is utilized as an image pre-processing tool for object detection tasks. The experimental results show that the EDN-GTM scheme can improve object detection accuracy by 4.7% and 1.2% in mAP on WAYMO and Foggy Driving datasets, respectively. From these results, we can conclude that the EDN-GTM scheme has promising potential to be an image pre-processing tool for practical driving object detection problems.

References

1. Li, B., Peng, X., Wang, Z., Xu, J., Feng, D.: AOD-Net: All-in-One Dehazing Network. In: IEEE International Conference on Computer Vision (ICCV), Italy, 22-29 Oct., 2017, pp. 4770-4778.
2. Meng, G., Wang, Y., Duan, J., Xiang, S., Pan, C.: Efficient Image Dehazing with Boundary Constraint and Contextual Regularization. In: 2013 IEEE International Conference on Computer Vision, Sydney, NSW, Australia, 1-8 Dec. 2013.
3. Zhu, Q., Mai, J., Shao, L.: A Fast Single Image Haze Removal Algorithm Using Color Attenuation Prior. IEEE Transactions on Image Processing, Volume 24, Issue 11, Nov. 2015, pp. 3522–3533.

4. He, K., Sun, J., Tang, X.: Single Image Haze Removal Using Dark Channel Prior. IEEE Transactions on Pattern Analysis and Machine Intelligence, Volume 33, Issue 12, Dec. 2011, pp. 2341–2353.
5. Cai, B., Xu, X., Jia, K., Qing, C., Tao, D.: DehazeNet: An End-to-End System for Single Image Haze Removal. IEEE Transactions on Image Processing, Volume 25, Issue 11, Nov. 2016.
6. Ren, W., Liu, S., Zhang, H., Pan, J., Cao, X., Yang, M.: Single Image Dehazing via Multi-Scale Convolutional Neural Networks. In: 2016 14th European Conference on Computer Vision (ECCV), Amsterdam, The Netherlands, October 11–14, 2016.
7. Dong, Y., Liu, Y., Zhang, H., Chen, S., Qiao, Y.: FD-GAN: Generative Adversarial Networks with Fusion-discriminator for Single Image Dehazing. In: Thirty-Fourth AAAI Conference on Artificial Intelligence, New York, USA, February 7-12, 2020.
8. Tran, L.-A., Moon, S., Park, D.-C.: A Novel Encoder-Decoder Network with Guided Transmission Map for Single Image Dehazing. In: International Conference on Industry Sciences and Computer Sciences Innovation (iSCSi), Porto, Portugal, 2022.
9. Ronneberger, O., Fischer, P., Brox, T.: U-Net: Convolutional Networks for Biomedical Image Segmentation. In: 18th International Conference on Medical Image Computing and Computer-Assisted Intervention (MICCAI 2015), Germany, October, 2015, pp. 234-241.
10. Bochkovskiy, A., Wang, C., Liao, H. M.: YOLOv4: Optimal Speed and Accuracy of Object Detection. arXiv preprint arXiv:2004.10934, 2020.
11. Ramachandran, P., Zoph, B., Le, Q.-V.: Searching for activation functions. arXiv preprint arXiv:1710.05941, 2017.
12. Godard, C., Mac Aodha, O., Firman, M., Brostow, G. J.: Digging into self-supervised monocular depth estimation. In: IEEE/CVF International Conference on Computer Vision, 2019, pp. 3828–3838.
13. Sun, P., Kretzschmar, H., Dotiwalla, X., Chouard, A., Patnaik, V., Tsui, P., Guo, J., Zhou, Y., Chai, Y., Caine, B. et al.: Scalability in perception for autonomous driving: Waymo open dataset. In: Proceedings of the IEEE/CVF Conference on Computer Vision and Pattern Recognition, 2020, pp. 2446–2454.
14. Zhang, H., Sindagi, V., Patel, V. M.: Multi-scale Single Image Dehazing Using Perceptual Pyramid Deep Network. In: 2018 IEEE/CVF Conference on Computer Vision and Pattern Recognition Workshops (CVPRW), Salt Lake City, UT, USA, 18-22 June 2018.
15. Wu, H., Qu, Y., Lin, S., Zhou, J., Qiao, R., Zhang, Z., Xie, Y., Ma, L.: Contrastive Learning for Compact Single Image Dehazing. In: IEEE/CVF Conference on Computer Vision and Pattern Recognition (CVPR), Virtual Conference, 2021, pp. 10551-10560.
16. Ancuti, C., Ancuti, C. O., De Vleeschouwer, C.: D-hazy: A dataset to evaluate quantitatively dehazing algorithms. In: 2016 IEEE international conference on image processing (ICIP). IEEE, 2016, pp. 2226–2230.
17. Sakaridis, C., Dai, D., Van Gool, L.: Semantic foggy scene understanding with synthetic data. International Journal of Computer Vision, vol. 126, no. 9, pp. 973–992, 2018.
18. Dong, H., Pan, J., Xiang, L., Hu, Z., Zhang, X., Wang, F., Yang, M.: Multi-Scale Boosted Dehazing Network with Dense Feature Fusion. In: 2020 IEEE/CVF Conference on Computer Vision and Pattern Recognition (CVPR), Seattle, USA, 2020, pp. 2157-2167.

19. Dudhane, A., Murala, S.: C2MSNet: A Novel Approach for Single Image Haze Removal. In: Winter Conference on Applications of Computer Vision (WACV-2018), Lake Tahoe, USA, 2018.
20. Ren, W., Pan, J., Zhang, H., Cao, X., Yang, M.-H.: Single image dehazing via multi-scale convolutional neural networks with holistic edges. International Journal of Computer Vision, vol. 128, no. 1, pp. 240–259, 2020.
21. Tran, L.-A., Le, M.-H.: Robust U-Net-based road lane markings detection for autonomous driving. In: International Conference on System Science and Engineering (ICSSE), Dong Hoi, Vietnam, 2019.